P1.2 OCEANIC CONVECTION DIAGNOSIS AND NOWCASTING

Cathy Kessinger*, Huaqing Cai, Nancy Rehak, Daniel Megenhardt,
National Center for Atmospheric Research, Boulder, CO

Jeffrey Hawkins, Richard Bankert
Naval Research Laboratory, Monterey, CA

Earle Williams
Massachusetts Institute of Technology Lincoln Laboratory, Lexington, MA

1. Introduction

The oceanic aviation community is hampered by a limited availability of accurate, high resolution products that depict the current and future locations of convective activity. Due to the scarcity of conventional in-situ observations, satellite remote sensing provides the only platform capable of monitoring convective cloud attributes near the temporal and spatial sampling required. In this National Aeronautics and Aviation and Administration (NASA) Earth Observing System (EOS)-sponsored program, an Oceanic Convection Diagnosis and Nowcasting system is under development that utilizes a diverse range of geostationary and polar-orbiting satellite observations plus global numerical model results to provide products for use by the oceanic aviation community. Products that depict the current convection location and give 1-hr or 2-hr nowcasts of convection location are shown over domains that include the Gulf of Mexico, the Pacific, and the CONUS with future expansion into the Atlantic planned. Near real-time products are placed on the World Wide Web at http://www.rap.ucar.edu/projects/ocn under the "Operations" sub-menu.

The Tropical Rainfall Measuring Mission (TRMM) Precipitation Radar (PR) and Lightning Imaging System (LIS) along with the CloudSat Cloud Profiling Radar (CPR) will provide a means to accurately validate the oceanic convection products. This work is an extension of the techniques described within Donovan et al. (in press).

* Corresponding author address: Cathy Kessinger, NCAR/RAL, 3450 Mitchell Lane, Boulder, CO 80301; email: kessinge@ucar.edu

2. Data Sets

The following data sets are currently being utilized by the Oceanic Convection Diagnosis and Nowcasting system.

- Geostationary Operational Environmental Satellite (GOES) East and West imagery
- Japan Civil Aviation Bureau (JCAB) Multifunction Transport Satellite-2 (MTSAT-2) imagery
- National Center for Environmental Prediction (NCEP) Global Forecasting System (GFS) numerical model
- QuikSCAT scatterometer near-surface wind vectors
- Advanced Microwave Scanning Radiometer (AMSR-E, Aqua)
- Advanced Microwave Sounding Unit (AMSU, Aqua and NOAA polar orbiters)
- Atmospheric Infrared Sounder (AIRS, Aqua)
- Moderate Resolution Imaging Spectroradiometer (MODIS, Aqua/Terra)
- Total Precipitable Water (TPW) product (SSM/I and AMSR-E)

Future data sets that will soon be utilized include the following.

- TRMM PR and LIS
- CloudSat CPR
- Satellite atmospheric motion vectors

A brief investigation into the near-surface, ocean wind vectors from the polar-orbiting Metop-A Advanced SCATteromter (ASCAT) radar suggests that these data could be ingested into the oceanic nowcasting system once the data are quality controlled by our team.. The ASCAT products were recently (October 2007) declared pre-operational. Fully-calibrated ASCAT backscatter data are expected in early 2008. These wind

vectors can be combined with the QuikSCAT wind vectors to enhance the temporal coverage of the near-surface oceanic winds.

3. Convective Diagnosis Oceanic

The Convective Diagnosis Oceanic (CDO) algorithm, as developed previously in collaboration with the Federal Aviation Administration (FAA) Aviation Weather Research Program (AWRP; Kessinger et al. 2006a), is used to detect the presence of convection in oceanic/remote regions and is briefly described here (see Kessinger et al. (2006b) for a full description of the CDO algorithm). Using a fuzzy logic, data fusion technique, outputs from three satellite-based convection detection algorithms are combined into the CDO. The three algorithms are the NRL cloud top height (CTOP; Donovan et al., 2008), the NRL cloud classification algorithm (CClass; Tag et al. 2000; Bankert and Aha, 1996) and the global convective diagnosis (GCD; Mosher 2002) algorithm.

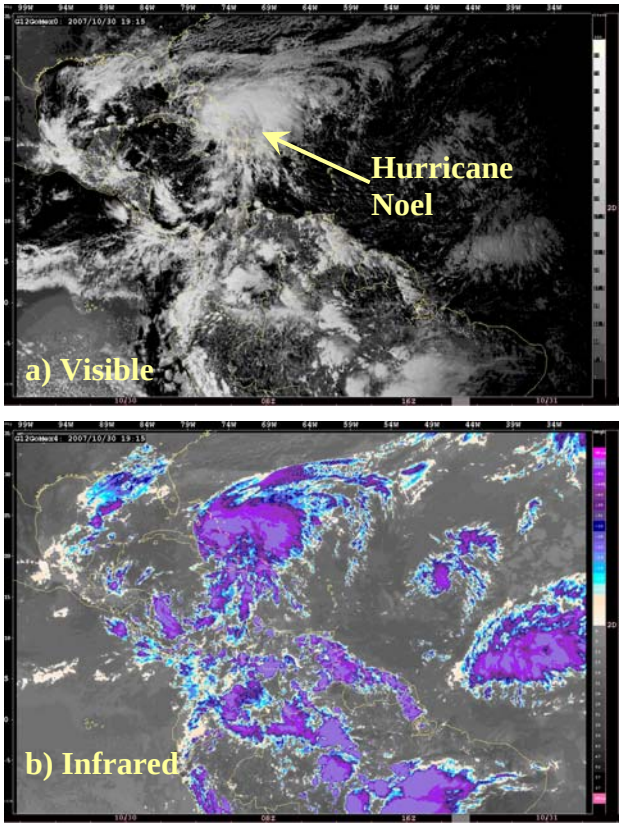

Figure 1. The GOES-12 a) visible and b) infrared imagery are shown from 30 October 2007 at 1915 UTC.

Hurricane Noel, located over eastern Cuba on 30 October 2007 at 1915 UTC (Fig. 1), is shown to illustrate the performance of the CDO during daytime hours. The previous day, Hurricane Noel had produced heavy rainfall over Haiti and the Dominican Republic with resultant flooding and mudslides and had caused the deaths of at least 80 people, according to a National Hurricane Center report. In Figure 1, the visible and infrared imagery from the GOES-12 satellite are shown. In Fig. 2, the three input fields (CTOP, CClass and GCD) for the CDO are shown; Hurricane Noel is resolved by all input fields.

After the fuzzy logic, data fusion technique for the CDO product is applied (not shown), the resultant interest field (shown in Fig. 3a) is produced where interest values range from 0 to 4. After the application of a threshold at "2.5 interest", the de-fuzzified, binary output of the CDO is produced and is shown in Figure 3b. For comparison purposes, the CDO output polygons are overlaid onto the cloud top height product to show their positive alignment (Fig. 3c).

A second, night-time case is shown from 16 October 2007 at 0045 UTC (Fig. 4) over the Gulf of Mexico domain. Similar to the previous case, Figure 4 shows the a) GOES-E infrared channel, b) the cloud top height output, c) the cloud classification output and d) the global convective diagnosis output. Figure 5 shows the resultant output of the CDO where the product is displayed over the cloud top height output; magenta-filled polygons denote regions of convective activity. Several regions of convection are apparent. Of particular interest is the region of convection that is to the south of Louisiana and Alabama that is approaching the CONUS (encircled with a red oval in all panels of Figures 4 and 5). As will be shown later, this region will experience convective initiation and growth in the next few hours. Cold front positions shown in all subsequent figures are determined from the Hydrometeorological Prediction Center (HPC) surface analysis products for the greater CONUS region.

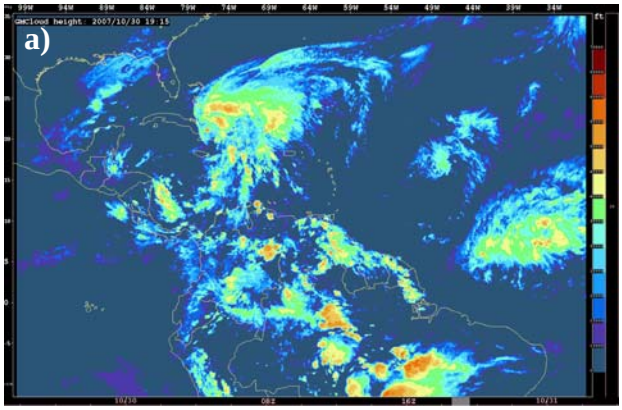

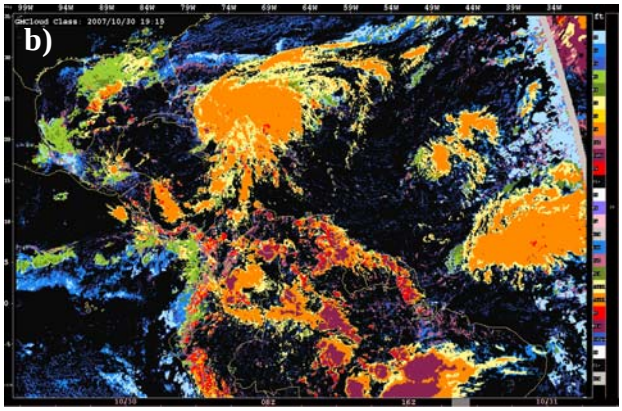

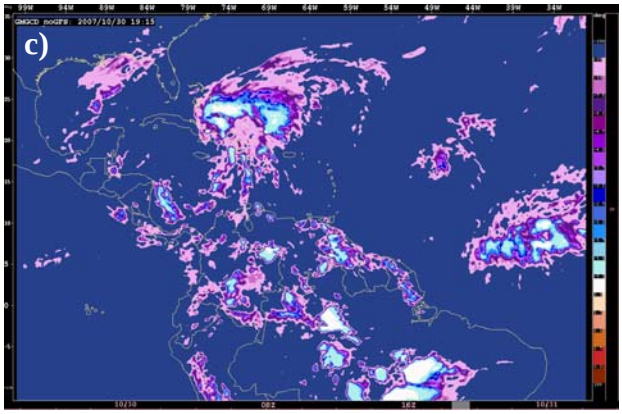

Figure 2. The input fields for the Convective Diagnosis Oceanic (CDO) algorithm are shown. In a) the NRL cloud top height (kft) is shown; in b) the NRL cloud classification algorithm is shown; and in c) the global convective diagnosis is shown. The date is 30 October 2007 at 1915 UTC.

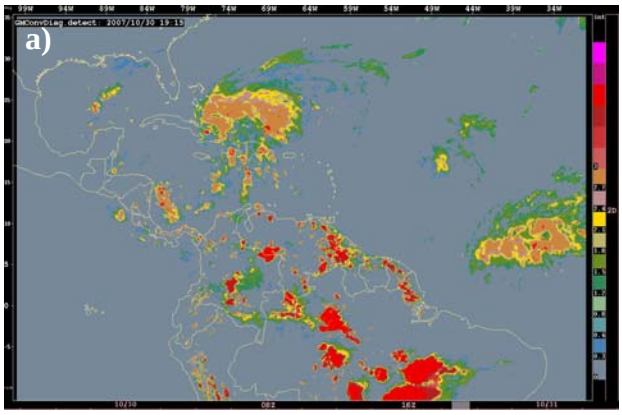

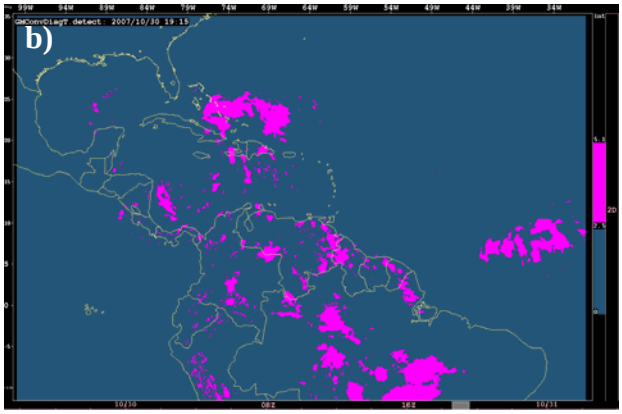

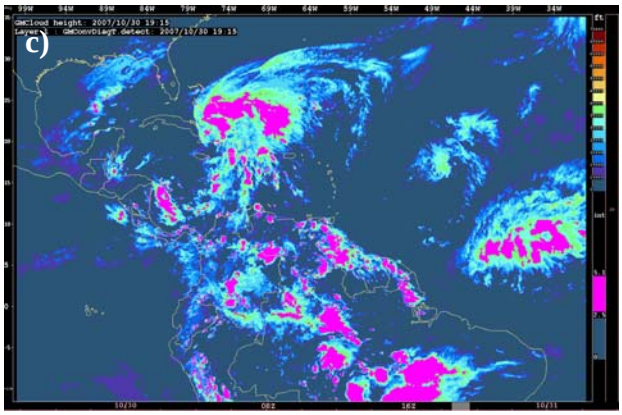

Figure 3. Resultant output from the CDO algorithm using the input fields shown in Figure 8. In a), all interest values of the CDO are shown. In b), a threshold is applied at 2.5 interest to create the binary field (magenta-filled contours) that indicate the presence of convective clouds. In c) the binary field is overlaid onto the cloud top height field for comparison purposes.

.

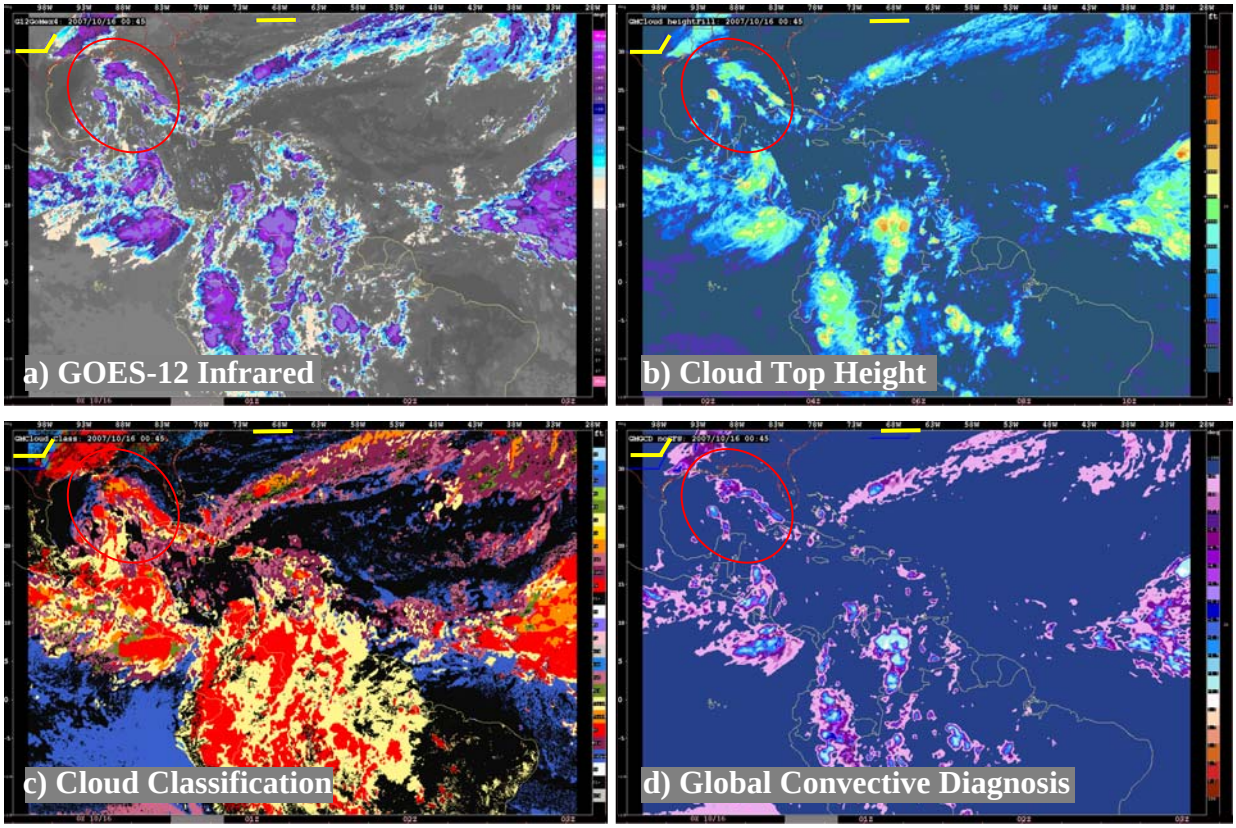

Figure 4. Data are shown from the a) GOES-12 infrared channel, b) the cloud top height product, c) the cloud classification product and d) the global convective diagnosis product for the Gulf of Mexico region. Data are taken from 16 October 2007 at 0045 UTC. Yellow lines in the upper left of each panel indicate the position of cold fronts within the CONUS. The region encircled by the red oval will undergo convection initiation over the next few hours.

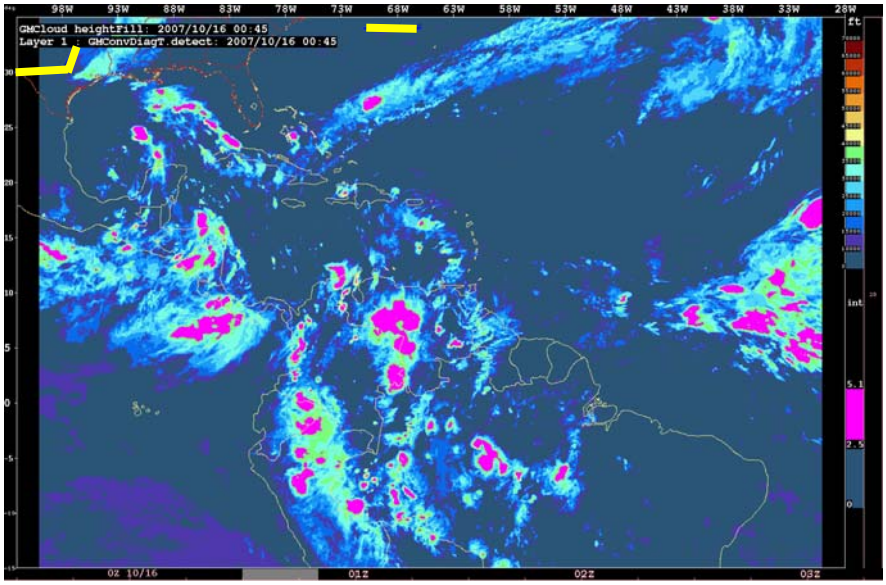

Figure 5. The output from the cloud top height algorithm is shown on 16 October 2007 at 0045 UTC with the thresholded output from Convective Diagnosis Oceanic (CDO) algorithm shown as magenta-shaded polygons. Yellow lines (in the upper left of the figure) indicate cold frontal positions in the CONUS.

4. Global Forecasting System Products

Megenhardt et al. (2004) used the Rapid Update Cycle (RUC) numerical model to compute derived fields called the "frontal likelihood" and the "stability analysis". The frontal likelihood product specifies the likelihood that a front exists at a particular location; the higher the value of the frontal likelihood, the more likely that a front is present. This field is derived from a fuzzy logic algorithm that utilizes horizontal convergence, vertical vorticity and the equivalent potential temperature (theta-e) gradient as its input fields. The stability analysis product specifies the number of layers where convective instability exists through a vertical column of the numerical model; therefore, the higher the value the more convectively unstable the atmosphere is at a given location. These fields should prove useful to oceanic regions as well, and, for this reason, a technology transfer was accomplished to perform the same calculations using the NCEP GFS model.

The frontal likelihood field on 16 October 2007 is shown at the 1000 mb level and at 0300 UTC in Fig. 6a with the position of the cold fronts (blue lines) also indicated. Notice the good correlation between the positions of the cold front across the southeastern CONUS with the higher values of the frontal likelihood field. The region that will undergo significant convection initiation (from Fig. 4) is also indicated. As shown by the frontal likelihood field, this region can expect larger scale forcing due to the presence of the cold front. In Fig. 6b, the pressure value at the ground's surface is shown from the GFS model to illustrate that additional quality control work is needed with the frontal likelihood field. For instance, the Andean mountains on the western coast of South America indicate high values of frontal likelihood (Fig. 6a) at 1000 mb while the surface pressure (Fig. 6b) is generally much lower in pressure (i.e., higher in altitude), meaning that the frontal likelihood is being calculated for grid points beneath the ground's surface. This additional quality control step will be added in the future.

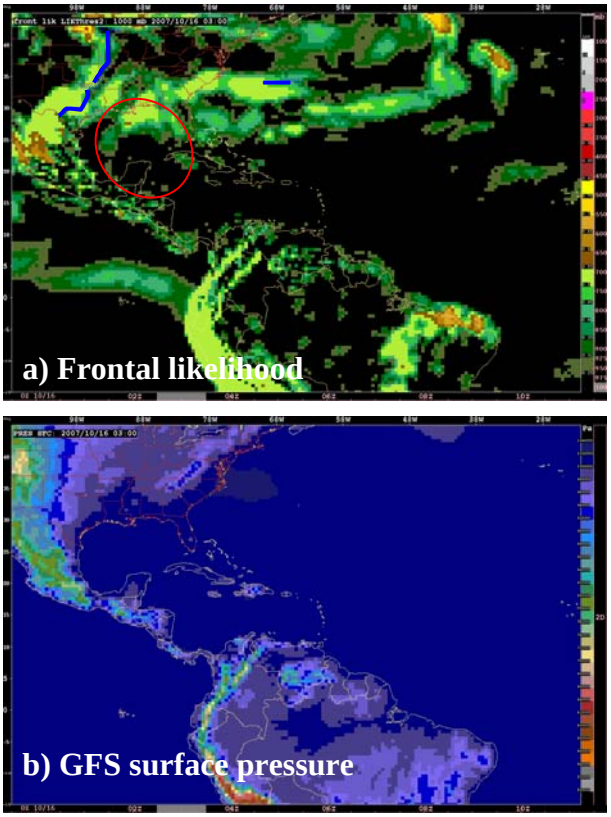

Figure 6. Fields shown are the a) frontal likelihood computed at the 1000 mb level at 0300 UTC on 16 October 2007 and b) the pressure level of the surface as determined by the GFS model. The HPC cold frontal positions in the CONUS are indicated by the dark blue lines.

The stability analysis field is shown in Fig. 7 for two times, at a) 0000 UTC and at b) 0600 UTC on 16 October 2007 to show the changes in the field, especially for the region of convection initiation discussed above and again indicated by the red oval. Within this region, notice that the stability field increases in value and becomes more organized over this 6 hour period. Examination of the cloud top height field (Fig. 8) at the times of 0045 UTC and 0715 UTC on this day shows convection initiation did occur within the region of interest. Clearly, the frontal likelihood and stability analysis fields will be important additions to the CNO as indicators for the potential for convective initiation.

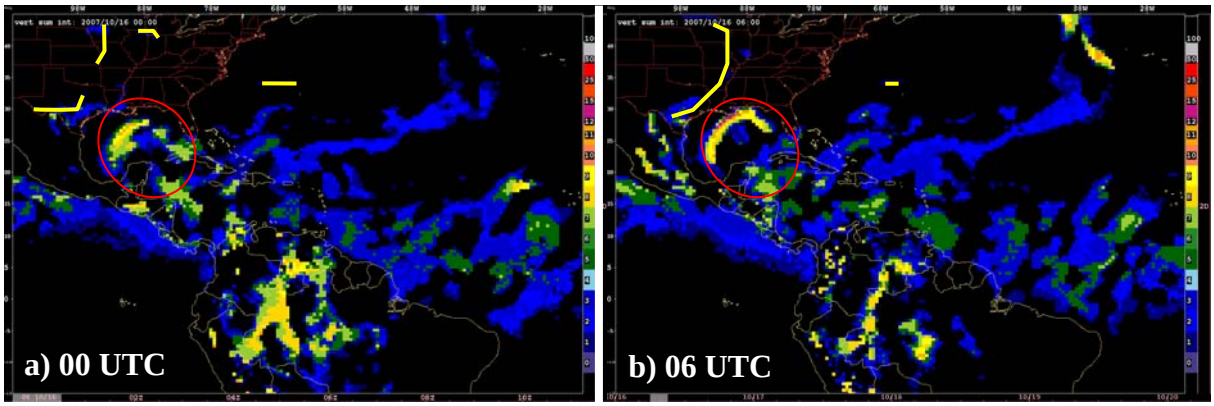

Figure 7. The stability analysis is shown for a) 0000 UTC and b) 0600 UTC on 16 October 2007. The red oval indicates the region of convection initiation. The yellow lines (upper left) indicate cold frontal positions in the CONUS.

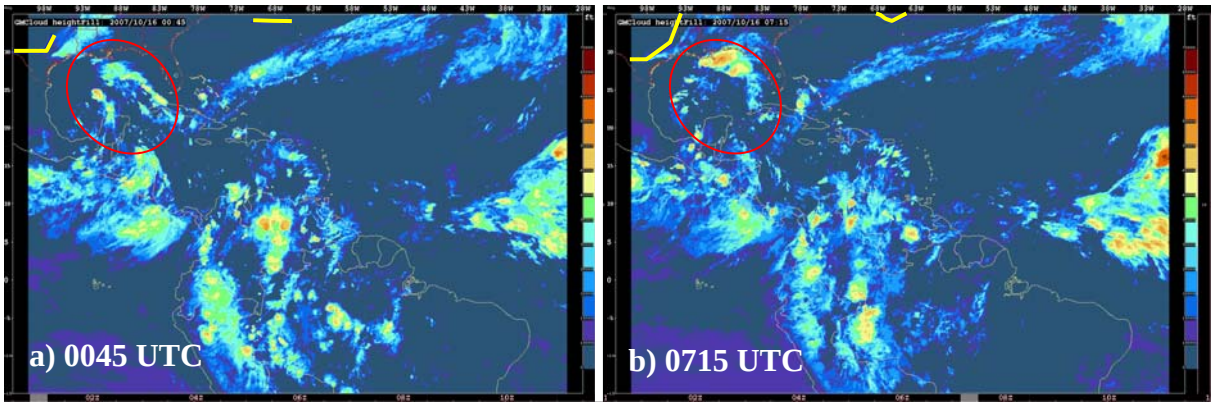

Figure 8. The cloud top height product is shown for two times: 0045 UTC and 0715 UTC on 16 October 2007 to illustrate the convection initiation that occurred within the regime encircled by the red oval. Cold frontal positions are indicated by yellow lines (upper left).

5. Convective Nowcasting Oceanic

Currently, the Convective Nowcasting Oceanic (CNO) product uses an object-tracker to extrapolate CDO-defined storms for 1 and 2 hours into the future and is called Thunderstorm Initiation, Tracking and Nowcasting (TITAN; Dixon and Wiener, 1993). The TITAN software uses a storm's previous history to project its future position and trend. The TITAN parameter files were tuned and an error in parameter setting was found and corrected, and resulted in greatly improved performance scores for extrapolation.

Figure 9 shows an example of the 1-hr and 2-hr storm position nowcasts overlaid as polygons onto the Convective Diagnosis Oceanic (CDO) output at the forecast validation time. The nowcast issue time was 0045 UTC (Fig. 5). Figure 9a shows the 1-hr storm extrapolation polygons issued at 0045 UTC with the CDO product at the verification time (0145 UTC) while Fig. 9b shows the same for the 2-hr storm extrapolations (0215 UTC verification time used since data from 0245 UTC were not available). As can be seen in the 1-hr and 2-hr nowcasts, the CNO frequently predicts the correct location of the convection but spatial offsets can and do occur.

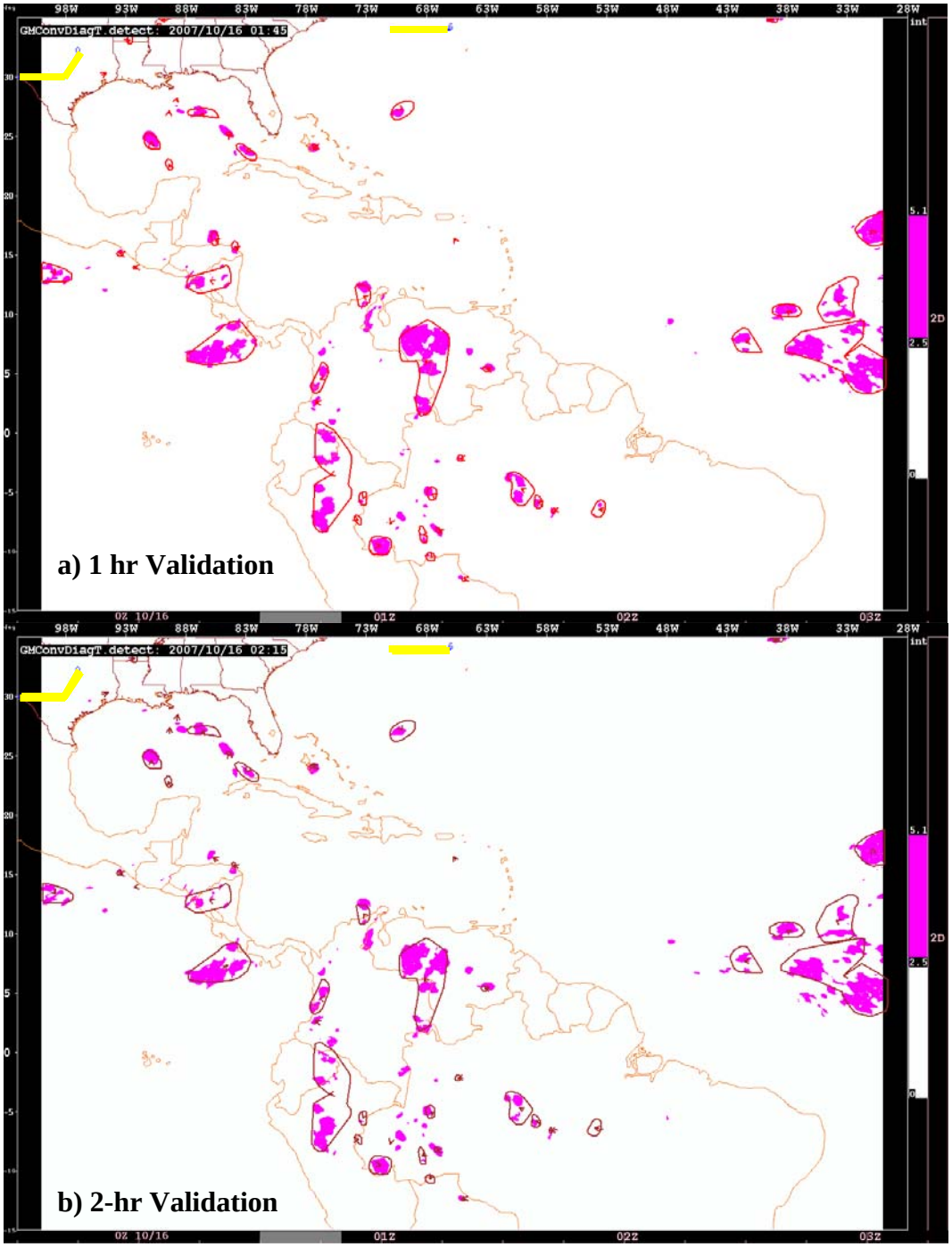

Figure 9. Output from the Convective Diagnosis Oceanic (CDO) algorithm is shown (magenta-filled polygons) at a forecast valid time of a) 0145 UTC and b) 0215 UTC using the data shown in Figs. 4 and 5 at the forecast issue time. Nowcast storm-positions from the TITAN storm tracking algorithm as issued at 0045 UTC are also indicated. In a) the 1-hr storm position nowcasts valid at 0145 UTC are indicated as red lines while in b) the 2-hr storm position nowcasts valid at 0245 UTC are indicated as dark brown lines. The 0245 UTC satellite imagery was not available; therefore the 0215 UTC imagery is shown. The yellow lines indicate HPC cold front positions in the CONUS at forecast issue time.

Work in-progress includes the characterization of the oceanic environment (Cai et al. 2008) into the CNO system to add additional complexity over the object-tracking methodology of TITAN. TITAN can only extrapolate existing storms and has no ability to predict convection initiation. Inclusion of the oceanic environment information should set the stage for understanding where new convection may form, given the presence of a triggering mechanism. Initial consideration will be given to the use of fuzzy logic, data fusion techniques due to their relative ease of implementation.

However, another methodology called "random forest" is under consideration that is a powerful, non-linear statistical analysis technique. This technique is currently under investigation within the AWRP Convective Weather Research Team (Williams et al., 2008). A random forest consists of a collection of independent decision trees that are produced from a "training set" of predictor variables paired with their corresponding set of "truth" values. Each decision tree's forecast logic is based on a random subset of data and predictor variables, making it independent from all others. A trained random forest functions as an "ensemble of experts" and uses a consensus vote to classify each new data point. Preliminary experiments suggest that the random forest technique may be quite useful.

6. Verification of Nowcasting Products

The TRMM Precipitation Radar (PR) and the Lighning Imaging System (LIS) along with the CloudSat Cloud Profiling Radar (CPR) will be used to validate the oceanic convection products. The automated, validation technique described by Donovan et al (2008) will be revised and the CloudSat CPR added. This work will be an important addition to the CNO as it will show the quality of the nowcast predictions within an oceanic environment.

7. Characterization of Oceanic Convection

An effort is underway to better understand the nature of environmental factors that contribute to oceanic convection initiation, development and dissipation (Cai et al. 2008). Once the nature of the contribution is known, the Convective Nowcasting Oceanic (CNO) system can include these features to better predict the initiation, growth and dissipation of oceanic convection. Various data sets, described below, will be incorporated into the CNO to accomplish this.

6.1 Sea surface temperature

The Aqua AMSR-E sea surface temperature (SST) data are ingested over the Gulf of Mexico domain (Fig. 10) and are interpolated to a latitude/ longitude grid with a resolution of 0.2 degrees (approximately 20 km). Multiple swaths from Aqua are accumulated to fill the region with SST values. The data values at a grid point are replaced when either new data becomes available or are set to "missing" when the expiration time of up to 24 hours is reached. Quality control procedures are implemented to remove precipitation and landmass contamination. As Fig. 10 shows, some temperature variation can be seen from swath to swath and likely indicates the diurnal temperature variation of the SST.

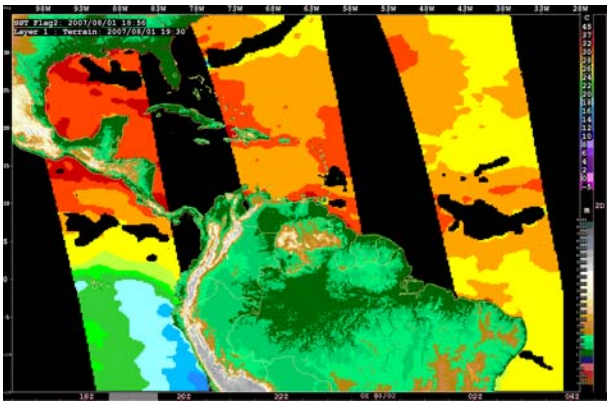

Figure 10. Sea surface temperature (^{o}C) is shown for the Gulf of Mexico domain on 3 August 2007. Multiple satellite swaths are overlaid to create a nearly continuous field. Precipitation contamination has been removed from the field.

Work in progress is to evaluate the SST in regions where convection initiates.

Future work is to expand the domain of coverage for the SST product into a global domain. To fill in SST data gaps created during the quality control process, a background SST field from other sources will be added. Possible sources of the background data could include gridded SST data from the National Oceanic and Atmospheric

Administration (NOAA) or a "blended" microwave/IR SST product available from NRL via Remote Sensing Systems.

6.2 QuikSCAT derived fields

The QuikSCAT near-surface wind data are interpolated to a latitude/longitude grid with a grid resolution of 0.25 degrees. Quality control of the data fields utilizes the rain flag for removal of precipitation-contaminated winds. Figure 11a shows the accumulated wind speed from QuikSCAT where multiple swaths are overlaid. The data are retained for 12 hours and replaced when either new data are available or when the expiration time is reached. Derived fields such as divergence/convergence (Fig. 11b) and vertical vorticity (Fig. 11c) are calculated. Merger with the near-surface winds from the Global Forecasting System (GFS) numerical model has been accomplished but the appropriate spatial filter remains under development. Without the appropriate filter, discontinuities are introduced during the merger of the model winds and the QuikSCAT winds such that artifacts are created. This work is under development.

Work in progress is to include the QuikSCAT winds into the CNO as an indicator for the location of low-level convergence boundaries as a potential triggering mechanism for convection.

6.3 AIRS derived fields

The AMSU and AIRS retrieved temperature and moisture soundings are produced at NRL/Fleet Numerical Meteorology and Oceanography Center (FNMOC). A latitude/longitude map projection is used with a grid resolution of 0.5 degrees. Various indicators such as the Convective Available Potential Energy (CAPE; Fig. 12) are computed. Swaths are accumulated over a 12 hour period to fill the Gulf of Mexico region; the data within a grid point are replaced with new data as it becomes available or are aged off when the expiration time (12 hrs) is reached.

In Figure 12, a comparison is made between the AIRS/AMSU derived CAPE values at 925 mb and the GFS model CAPE values at the same vertical level. While the AIRS/AMSU CAPE values generally have a similar trend as the GFS (i.e., both have maxima near the same location), the

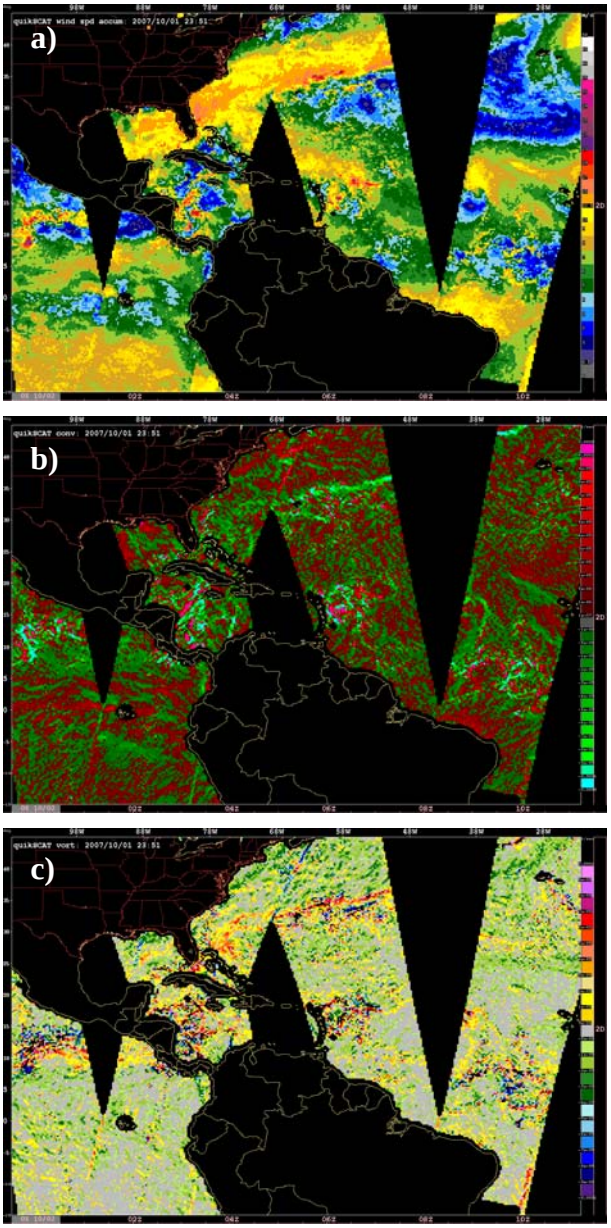

Figure 11. Accumulated QuikSCAT fields are shown for the Gulf of Mexico domain on 1 October 2007 over the 12 hour period ending at 2351 UTC. The wind speed (m s^{-1}) is shown in a) with the b) horizontal convergence (s^{-5}) and the c) vertical vorticity (s^{-5}).

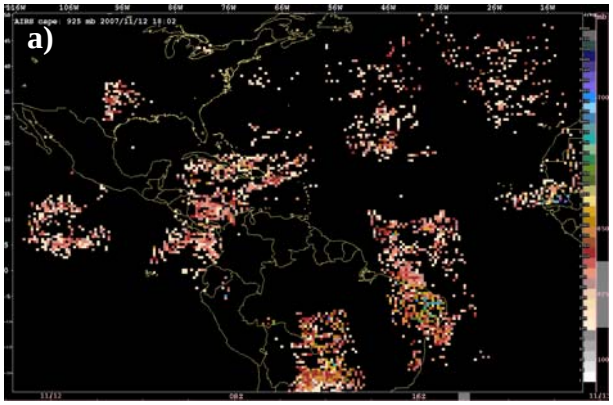

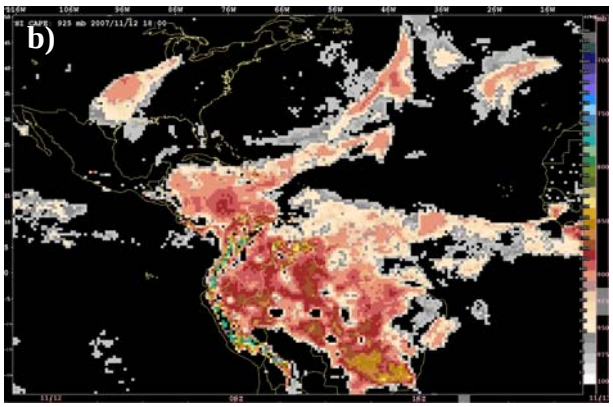

Figure 12. The Convective Available Potential Energy (CAPE) field (j/kg) is shown at 925 mb as derived from the a) AIRS/AMSU soundings for the Gulf of Mexico region on 12 November 2007 for the 12 hour period ending at 1802 UTC. In b), the corresponding GFS CAPE values are shown as computed at 925 mb at 1800 UTC.

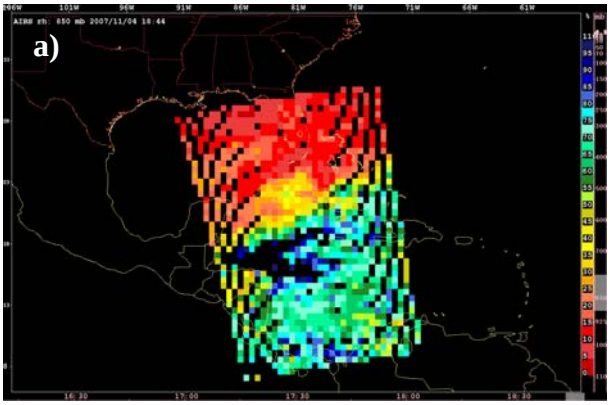

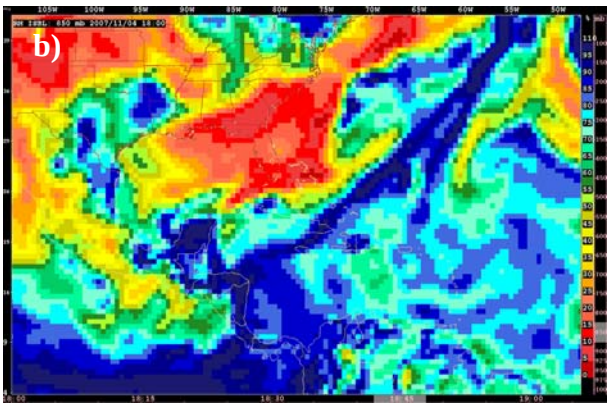

Figure 13. The 850 mb relative humidity field is shown as retrieved from a) the AIRS/AMSU soundings at 1844 on 4 November 2007 and in b) by the GFS model at 1800 UTC of the same day. Warm colors indicate dry conditions; cool colors indicate moist conditions.

AIRS/AMSU values tend to be higher than the GFS values. This difference will be investigated to ascertain the cause.

A comparison was made between radiosonde thermodynamic data from two stations in Mexico to the AIRS/AMSU thermodynamic data when both datasets were close in space and time. General agreement between the AIRS/AMSU and the radiosonde data was found, with a temperature difference of less than approximately 3^{o}C and relative humidity difference of less than approximately 30% in a worst case scenario.

Merger with particular GFS fields is accomplished using a point replacement technique when the data are within specified temporal limits (generally 12 hours). An example is shown in Figure 13 for the 850 mb relative humidity on 4 November 2007. The AIRS/AMSU relative humidity data at 1844 UTC (Figure 13a) are compared to the GFS relative humidity data from the 1800 UTC model results (Figure 13b). Comparing the two suggests that the AIRS/AMSU data have somewhat higher values than the GFS. Model results from 1200 and 0600 UTC (not shown) were examined but they showed very similar structures as the 1800 UTC results. Further investigation into possible reasons for the high bias is planned.

Work is in progress to incorporate the sounding and derived indices into the CNO to indicate regions where convective instability is/is not possible.

6.4 Total Precipitable Water

The total precipitable water (TPW) field gives information into the presence or absence of atmospheric water vapor and should prove to be a

valuable addition to the CNO system. The goal of using a TPW product is to ascertain whether the area of concern has enough moisture to support convection or whether dry air has been advected into the area possibly from a mid-latitude source or due to Saharan Air Layer (SAL) events that can impact the Gulf of Mexico region.

The nonlinear global algorithms are applied to each of the data sets (SSM/I and AMSR-E) and use a combination of similar channels for retrieval of TPW (Alishouse et al., 1990; Wentz and Meissner, 2000). The SSM/I channels are 19V, 22V, and 37V GHz and the AMSR-E channels are 18.7, 23.8, and 36.5 GHz. The final product is a simple blending of the TPW values from the two sensors. The TPW field is accurate to approximately a few millimeters. These NRL-derived TPW fields include 6-, 12- , and 24-hour composites. Six-hour composites are values from the latest retrieval in that time period. The 12 and 24-hour composites represent an average TPW value for each pixel over that time period. The 24-hour composite data sets are updated once per day. Rain masks are not applied.

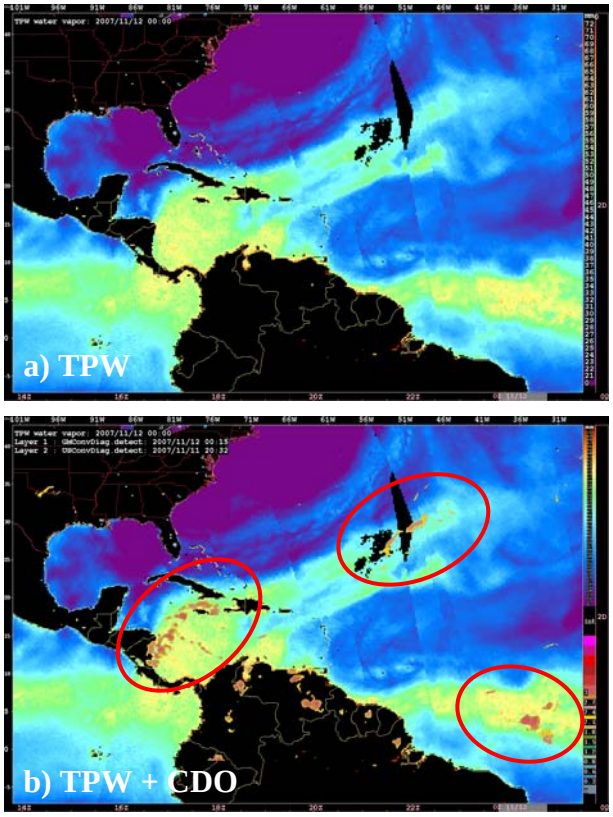

Figure 14. Data are shown for the TPW field on 12 November 2007 at 0000 UTC. The field is shown by itself in a) and in b) the field is overlaid with the thresholded output from the CDO algorithm. Regions of convection are indicated with red ovals. Warmer colors indicate higher values of TPW (i.e., moist conditions) while cooler colors indicate drier conditions.

The TPW data are interpolated to a latitude/ longitude grid with a resolution of 0.2 degrees. An example product is shown in Fig. 14. The TPW data are shown in a) by itself and in b) with the CDO product overlaid. In this example, the CDO is found within regions with higher TPW values, generally in excess of 30-40 mm.

This field is a very recent addition to the project. Work is planned to incorporate this field into the CNO system such that it will serve as a positive (negative) indicator for the potential for convective activity to be present (absent).

8. Web Site

The Oceanic Convection Diagnosis and Nowcasting web site is located at http://www.rap.ucar.edu/projects/ocn. Oceanic convection products are displayed in real-time on the web site under the "Operations" sub-menu on the home page. Here, the user can select the cloud top height product for various domains that includes the Gulf of Mexico, the continental United States (CONUS), as well as the South and North Pacific regions. Additional regions of interest to the oceanic aviation community are shown and include Hawaii, the GOES-West domain and the MTSAT domain. The addition of a domain covering the GOES-East region is planned. The Convective Product Suite is also available on the Operations sub-menu for the Gulf of Mexico and the CONUS domains, with expansion into the Pacific planned. The Convective Product Suite includes those fields developed under NASA sponsorship as well as the legacy products developed under FAA AWRP sponsorship. Static products are updated in near real-time as data sets become available.

9. Summary

The Oceanic Convection Diagnosis and Nowcasting project is working toward developing high resolution, satellite-based convective products

for the oceanic aviation community. These products are displayed on the World Wide Web in near real-time over several oceanic domains. With projected increases in the numbers of oceanic air flight, improved convective products will be needed for better enroute planning and avoidance of hazardous convection.

Oceanic convection is detected using a fuzzy logic, data fusion of three satellite-based algorithms. Convective nowcasts for 1-hr and 2-hr are calculated by using an object-based tracking system to extrapolate existing storms. Through the incorporation of environmental factors, as observed by polar-orbiting satellites from NASA EOS and others, additional information will be gleaned to ascertain potential areas for convection initiation as well as convective growth and/or dissipation.

10. Acknowledgements

This research is sponsored by the NASA Earth Observing System, in response to NRA #NNH05ZDA001N, Research Opportunities in Space and Earth Sciences (ROSES-2005). The material within is based upon work supported by NASA under award No. NNA07CN14A. Any opinions, findings and conclusions or recommendations expressed in this material are those of the authors and do not necessarily reflect the views of the National Aeronautics and Space Administration.

11. References

Alishouse, J., S. Snyder, J. Vongsathorn, and R. Ferraro, Determination of oceanic total precipitable water from the SSM/I, *IEEE Trans. Geosci. Remote Sens.*, **28**, 811-816, 1990.

Bankert, R. L., and D. W. Aha, 1996: Improvement to a neural network cloud classifier. *J. Appl. Meteor.*, **35**, 2036-2039.

Bankert, R.L. and R.H. Wade, 2007: Optimization of an instance-based GOES cloud classification algorithm. *J. Appl. Meteor.*, **46**, 36-49.

Cai, H., C. Kessinger, N. Rehak, and D. Megenhardt, 2008: Investigations of environmental conditions for storm initiation over the ocean using satellite data. *13th Aviation, Range and Aerospace Meteorology Conference,* American Meteorological Society, New Orleans, LA, 21-24 Jan 2008.

Dixon, M., and G. Wiener, 1993: TITAN: Thunderstorm Identification, tracking, Analysis and Nowcasting - A radar-based methodology. *J. Atmos. Oceanic Technol.*, **10**., 785-797.

Donovan, M.F., E.R. Williams, C. Kessinger, G. Blackburn, P.H. Herzegh, R.L. Bankert, S. Miller and F.R. Mosher, 2008: The identification and verification of hazardous convective cells over oceans using visible and infrared satellite observations. *J. Appl. Meteorology in press*.

Kessinger, C., P. Herzegh, G. Blackburn, R. Sharman, G. Wiener, B. Hendrickson, K. Levesque, J. Craig, T. Tsui, J. Hawkins, R. Bankert, E. Williams, M. Donovan, G. Ellrod, R. Kistler, and D. Fleming, 2006a: The FAA AWRP Oceanic Weather Product Development Team. *12th Aviation, Range and Aerospace Meteorology Conference*, American Meteorological Society, Atlanta, GA, 30 Jan-2 Feb 2006.

Kessinger, C., C. Mueller, H. Cai, G. Blackburn, N. Rehak, K. Levesque, b. Hendrickson, S. Carson and D. Megenhardt, 2006b: Oceanic Convection Diagnosis and Nowcasting. *5th International Conference on Mesoscale Meteorology and Typhoon*, East Asia Weather Research Association, Boulder, CO, 31 Oct-3 Nov 2006. http://www.eol.ucar.edu/icmcs/program.html (Tuesday session)

Megenhardt, D., C. Mueller, S. Trier, D. Ahijevych, and N. Rehak, 2004: NCWF-2 Probabilistic Nowcasts. *Preprints, 11th Aviation, Range and Aerospace Meteorology Conference*, American Meteorological Society, Hyannis, MA, 4-8 October 2004.

Mosher, F., 2002: Detection of deep convection around the globe. *Preprints, 10th Conference on Aviation, Range, and Aerospace Meteorology*, American Meteorological Society, Portland, OR, 289-292.

Tag, P. M., R. L. Bankert, and L. R. Brody, 2000: An AVHRR multiple cloud-type classification package. *J. Appl. Meteor.*, **39**, 125-134.

Wentz, F. and T. Meissner. 2000. AMSR-E Ocean Algorithm. *Algorithm Theoretical Basis*

Document, Version 2. Santa Rosa, CA, USA: Remote Sensing Systems.

Williams, J.K., D.A. Ahijevych, C.J. Kessinger, T.R. Saxen, M. Steiner, and S. Dettling, 2008: A machine learning approach to finding weather regimes and skillfull predictor combinations for short-term storm forecasting. *13th Aviation, Range and Aerospace Meteorology Conference*, American Meteorological Society, New Orleans, LA, 21-24 Jan 2008.